# JCI insight

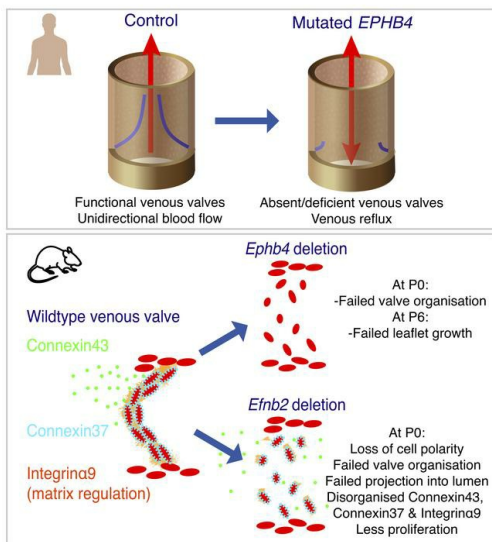# Mutations in *EPHB4* cause human venous valve aplasia

Oliver Lyons, … , Prakash Saha, Alberto Smith

**Research** In-Press Preview **Angiogenesis** **Development**

## Graphical abstract

**Title: Mutations in *EPHB4* cause human venous valve aplasia**

**Running Title: Venous valve aplasia**

**Authors**

Oliver Lyons[1*], James Walker[1], Christopher Seet[1], Mohammed Ikram[1], Adam Kuchta[2], Andrew Arnold[2], Magda Hernandez-Vasquez[3], Maike Frye[3], Gema Vizcay-Barrena[4], Roland A. Fleck[4], Ash Patel[1], Soundrie Padayachee[2], Peter Mortimer[5], Steve Jeffery[5], Siren Berland[6], Sahar Mansour[5,7], Pia Ostergaard[5], Taija Makinen[3], Bijan Modarai[1], Prakash Saha[1], Alberto Smith[1*]

**Affiliations**

1. Academic Department of Vascular Surgery, School of Cardiovascular Medicine and Sciences, BHF Centre of Research Excellence, King's College London, St Thomas' Hospital, London, United Kingdom
2. Department of Ultrasonic Angiology, Guy's & St Thomas' NHS Foundation Trust, London, United Kingdom
3. Rudbeck Laboratory, Department of Immunology, Genetics and Pathology, Uppsala University, Sweden
4. Centre for Ultrastructural Imaging, King's College London, London, United Kingdom
5. Molecular and Clinical Sciences Research Institute, St George's University of London, London, United Kingdom
6. Department of Medical Genetics, Haukeland University Hospital, Bergen, Norway
7. South West Thames Regional Genetics Service, St George's Hospital, London, United Kingdom

The authors have declared that no conflict of interest exists.

**Corresponding authors**

Dr Oliver Lyons & Prof Alberto Smith
Academic Department of Vascular Surgery, King's College London
1st Floor North Wing
St Thomas' Hospital
London, SE1 7EH
United Kingdom,
Email: oliver.lyons@cdhb.health.nz, alberto.smith@kcl.ac.uk Tel: +44(0)2071880214

Word count: 10 044 including abstract, references and main figure legends.

**Subject terms** Vascular Disease, Animal Models of Human Disease, Basic Science Research, Developmental Biology, Vascular Biology, Genetically Altered and Transgenic Models, Ultrasound

**Abstract:**

Venous valve (VV) failure causes chronic venous insufficiency, but the molecular regulation of valve development is poorly understood. A primary lymphatic anomaly, caused by mutations in the receptor tyrosine kinase *EPHB4,* was recently described, with these patients also presenting with venous insufficiency. Whether the venous anomalies are the result of an effect on VVs is not known. VV formation requires complex 'organization' of valve-forming endothelial cells, including their reorientation perpendicular to the direction of blood flow. Using quantitative ultrasound we identified substantial VV aplasia and deep venous reflux in patients with mutations in *EPHB4*. We used a GFP reporter, in mice, to study expression of its ligand, ephrinB2, and analysed developmental phenotypes following conditional deletion of floxed *Ephb4* and *Efnb2* alleles. EphB4 and ephrinB2 expression patterns were dynamically regulated around organizing valve-forming cells. *Efnb2* deletion disrupted the normal endothelial expression patterns of the gap junction proteins connexin37 and connexin43 (both required for normal valve development) around reorientating valve-forming cells, and produced deficient valve-forming cell elongation, reorientation, polarity, and proliferation. *Ephb4* was also required for valve-forming cell organization, and subsequent growth of the valve leaflets. These results uncover a potentially novel cause of primary human VV aplasia.

**Introduction**

Unidirectional blood flow requires functional venous valves (**VV**s) which are widely distributed throughout human veins and venules, predominantly in vessels less than 100µm in diameter.(1) Lower limb VVs are typically bicuspid and situated just upstream of the confluence with a tributary.(1, 2) Failure of these valves is the central feature of the venous reflux that is seen in up to 40% of adults,(3, 4) while congenital venous valve aplasia has also been identified.(5-8) In the lower limbs, venous reflux causes chronic venous hypertension, leading to pain, oedema, hyperpigmentation, skin damage, and chronic intractable ulceration.(3, 9, 10) Our understanding of the molecular mechanisms of VV embryological development, maintenance after formation, and failure in disease is limited, and there are few therapeutic options to treat VV dysfunction.(3, 11-16) Elucidating these mechanisms and understanding how their dysfunction may lead to VV failure could facilitate the development of novel therapies.

Clinical studies have suggested a link between venous reflux and some primary lymphedemas, and we have previously shown striking human VV disease in patients with primary lymphedema caused by mutations in *FOXC2* (MIM 602402) and *GJC2* (MIM 608803*).*(11, 17-20) Other human genetics studies have shown that mutations in the gene encoding the tyrosine kinase receptor EPHB4 (*EPHB4,* MIM 618196)*,* cause capillary malformation-arteriovenous malformation syndrome (CM-AVM2, including hereditary haemorrhagic telangiectasia and vein of Galen malformations, cutaneous malformations and arteriovenous malformations) and a primary lymphatic anomaly which includes clinical features such as central conduction lymphatic

97    anomaly, non-immune fetal hydrops, and atrial septal defects. (21-28). Patients with

98    the primary lymphatic anomaly were also reported to present with varicose veins and

99    early onset venous stasis.(21, 25, 28) In mice, early embryonic deletion of *Ephb4* in

100   lymphatic endothelia leads to subcutaneous oedema and abnormal dermal and

101   mesenteric lymphatic vasculature, whereas deletion in adult blood endothelia results

102   in coronary abnormalities including capillary microhaemorrhages.(21, 29)

103

104   The Eph's are the largest family of mammalian receptor tyrosine kinases and bind to

105   ephrins, their trans-cellular ligands.(30, 31) Cell-cell signaling may occur in either

106   direction, resulting in cell and context-specific effects, and is involved in regulating

107   many developmental processes including cell sorting and boundary formation.(32-34)

108   In the cardiovascular system ephrinB2 is widely accepted as an arterial-specific

109   marker, whereas EphB4 is used as a marker of venous endothelia.(35-37) EphrinB2-

110   EphB4 signaling is essential for developmental angiogenesis, and global knockout of

111   *Ephb4* is phenotypically similar to knockout of *Efnb2*, with both resulting in vascular

112   remodeling defects and embryonic lethality.(35, 38-40) Constitutive overexpression

113   of ephrinB2 leads to defects including abnormal intersomitic vessel patterning, aortic

114   dissection and aneurysm formation, and early neonatal lethality due to aortic

115   rupture.(41)

116

117   Signaling between ephrinB2 and EphB4 is required for lymphatic valve (**LV**)

118   development and maintenance, and for formation of valves at lymphovenous

119   junctions at the base of the neck.(12, 21, 42) LV cells fail to take on normal

120   morphology in *Efnb2*$^{\Delta V/\Delta V}$ mice (lacking the C-terminal PDZ interaction site), and it

121   was suggested that ephrinB2-EphB4 signaling is required to guide endothelial cell

122 (**EC**) migration and elongation during LV morphogenesis.(42) Blocking the forward

123 signaling activity of EphB4 results in failure of LV formation.(43, 44) Defects in

124 cardiac valve (**CV**) development leading to early perinatal death are found in

125 *Efnb2^βgal/βgal* mice, in which the cytoplasmic tail of ephrinB2 is replaced with βgal.(45)

126 In both LV and CV, the morphological effects of loss (or inhibition) of ephrinB2-

127 EphB4 signaling on Prox1^hi valve-forming cells (**VFCs**) remain unclear. Ephrin-Eph

128 interactions result in rapid changes in cellular direction and motility, leading to

129 boundary formation within initially mixed populations of cells (for example, in

130 mesenchymal cells), and can inhibit communication via gap junctions across these

131 boundaries.(31, 32, 46) In vitro, ephrinB2-EphB4 signaling controls EC repulsion and

132 segregation, leading to clustering of EphB4- or ephrinB2-expressing cells, akin to in

133 vivo boundary formation, but to the best of our knowledge this behaviour has not

134 been observed in ECs in vivo.(47)

135

136 We previously showed that ephrinB2 is required for postnatal VV leaflet development

137 and maintenance, but the expression of ephrinB2 and EphB4, and any roles in the

138 early organization of VFCs, have not been examined.(11, 12) In this study, we show

139 that mutations in *EPHB4* cause striking human VV disease, with an almost complete

140 loss of VVs seen in some patients. Given the known roles for ephrin-Eph interactions

141 in boundary formation in other tissues, we hypothesised that ephrin-Eph interactions

142 could regulate early organizational events in VV formation. We have therefore

143 focused on their respective roles in the regulation of the complex series of events

144 during early valve formation in mice, which includes the organization of a set of

145 Prox1^hi VFCs to form a ring of cells within the three-dimensional lumen of the vessel

146 (stage 1 of development).(11, 12) At P0 this structure is found predominantly on the

147  anterior vein wall, and then extends posteriorly.(11) Using a GFP reporter we

148  identified *Efnb2* expression within veins at the site of VV formation, and that the

149  organization of VFCs occurs at a striking boundary between venous ECs that

150  express ephrinB2 and those that do not. A conditional loss-of-function genetic

151  approach has enabled us to show that both ephrinB2 and EphB4 are required for

152  these early organizational events and that EphB4 is required for postnatal VV

153  development.

154

155

## Results

### *Patients with mutations in EPHB4 have fewer VVs and show deep venous reflux*

Pathogenic mutations in *EPHB4* were recently described in two families with primary lymphatic related fetal hydrops (LRFH), with autosomal dominant inheritance.[21] Adults in both families had a notably early onset of lower limb venous disease. We therefore characterised the numbers of valves per vein in these patients (N=5) and an unaffected relative using ultrasonography, and compared these results to a control population (N=12, Supplementary Table 1). VVs were readily detected in the unaffected relative and other controls, but fewer VVs were detected in patients carrying a heterozygous mutation in *EPHB4,* including three patients with a mosaic mutation in *EPHB4* (fold change 0.2 ±SD 0.29 for mosaic carriers, and 0.17±0.36 for constitutive carriers, $P=1.7 \times 10^{-11}$, ANOVA: F=30.3, 2df, Figure 1A,B, and Supplementary Figure 1). 92 veins were analysed in 13 controls, and 40 veins were analysed in 5 mosaic or constitutive *EPHB4* mutation carriers. Given the substantial loss of VVs in those with constitutive *EPHB4* mutations, too few VVs were available for detailed analysis of leaflet length in constitutive mutation carriers, but those VVs that were identified were not significantly shorter than controls (Supplementary Figure 1, fold change 1.15±0.63 for mosaic carriers, and 0.67±0.48 for constitutive carriers, P= not significant).  Groups were matched for age and sex (P= not significant). Those carrying an *EPHB4* mutation had a mean popliteal reflux duration of 1.37s, above the accepted diagnostic threshold of 1s for severe deep venous reflux. Both patients with constitutive *EPHB4* mutations exhibited a mean popliteal vein reflux duration ≥1s (Figure 1C,D, Supplementary Figure 1).

181

**_EphB4 is expressed at E18 and P0 and is required for normal VFC organization_**

EphB4 is the main ephrinB2 receptor in the vasculature, and these proteins often exhibit a complementary expression pattern during tissue segmentation.(13, 35) Our analysis initially focused on embryonic day 18 (E18) and postnatal day 0 (P0). We localised EphB4 expression in the region of the developing valve in _Efnb2$^{GFP}$_ mice, and then examined whether EphB4 is required for organization of VFCs at P0.

188

At E18, when VFCs are in the process of organizing themselves at the site of developing valves, EphB4 expression appeared to be stronger immediately upstream of areas showing VFC organization, and adjacent to VFCs with high _Efnb2_ expression (Figure 2A, Supplementary Figure 2C). Quantification of _Efnb2$^{GFP}$_ signal and EphB4 immunosignal across these organizing areas (yellow box in Figure 2A) confirmed relatively complementary expression with significantly higher EphB4 upstream and higher _Efnb2$^{GFP}$_ downstream of the VFCs (Figure 2B). Conversely, VFCs nearer the superior or inferior edges of the vessel already coexpressed _Efnb2$^{GFP}$_ and EphB4 (arrowheads in Figure 2A).

198

By P0, VFCs consistently reorientate and elongate to form a line of cells across the anterior femoral vein wall, and partly extend across the posterior wall, defined as stage 1 of VV development (schematic in Figure 2A). Prior to this, development is described as stage 0. We had thought that EphB4 expression would be complementary to _Efnb2_ expression at P0, but EphB4 was immunolocalised variably throughout the valve region, with stronger expression within clusters of VFCs at the superior and inferior regions of the valve (Figure 2C, arrowheads), where we

206  previously identified multiple proliferating VFCs.(11) Co-expression of Ephb4 and

207  *Efnb2* was confirmed in *Efnb2^GFP^* mice (Figure 2D and Supplementary Figure 2B).

208  Deletion of *Ephb4* at E15 resulted in disorganized VFCs at P0 (Figure 3A) albeit

209  some VVs developed normally to stage 1 (Figure 3B).

210

211  **Ephb4 is required for leaflet development to P6**

212

213  We next localised the expression of EphB4 in VV leaflets at P6 and in adult mice. We

214  then examined whether EphB4 is required for maturation of the valve leaflets up to

215  P6.

216

217  EphB4 continued to be expressed in the endothelia of veins and VV leaflets at P6

218  and in adults (Figure 3C, left panel). Expression was strongest on the lumen surface

219  of the valve leaflet, including cells at the free edge of valve leaflet (Figure 3C, right

220  panel). This expression is complementary to the previously identified lack of

221  expression of *Efnb2* in these free edge cells.(12) This could contribute to

222  maintenance of their phenotype, which is clearly different to the rounded morphology

223  of endothelia lining the sinus or lumen leaflet surfaces.(12)

224

225  At P6 VVs are normally at stages 3 or 4 (schematic in Figure 3), which were defined,

226  as previously, by the presence of one or two commissures.(11) Deletion of *Ephb4* at

227  P0 led to a complete failure of valve leaflet formation by P6, with only a few Prox1- or

228  Foxc2-expressing cells remaining (Figure 3D,E). This phenotype (*Ephb4* deletion at

229  P0, analysed at P6) was more consistent and severe than deletion at E15, analysed

230  at P0 (Figure 3A).

231

232  Similarly to other gene-deletion studies resulting in loss of VFCs by P6, there was an

233  associated failure to establish a local reduction in the density of smooth muscle cells

234  (SMCs) around the valve (Figure 3D).(11)

235

236  ***VFC organization occurs at a developing boundary between ECs expressing***

237  ***and not expressing Efnb2***

238

239  To visualise the *Efnb2* expression pattern during VFC organization we visualised the

240  site of VV formation in the proximal femoral vein using confocal microscopy of

241  wholemount samples from *Efnb2$^{GFP}$* reporter mice (Figure 4A). *Efnb2$^{GFP}$* signal was

242  strong in femoral artery ECs (Figure 4A, FA), and generally absent or at very low

243  levels in venous endothelia in all samples analysed, similar to previously reported

244  findings.(36, 37) Expression of *Efnb2* by venous smooth muscle α-actin-expressing

245  mural cells was not detected (data not shown). Global heterozygous knockout of

246  *Efnb2* (in the *Efnb2$^{GFP}$* reporter) did not prevent development of stage 1 VVs by P0

247  (P = NS vs wildtype littermates, N=32 *Efnb2$^{GFP/wt}$* VVs analysed). At E18 the

248  patterning of Prox1$^{hi}$ VFCs within the valve-forming region was more variable than at

249  P0, with areas of Prox1$^{hi}$ cells (e.g. the superior but not inferior area) showing

250  organization (i.e. reorientation and elongation of cells, Figure 4A, upper panel vs

251  lower panel). The organizing VFCs, and endothelia just downstream of organizing

252  VFCs, expressed *Efnb2* (Figure 4A, green box), whilst areas without VFC

253  organization did not develop a boundary in ephrinB2 expression (Figure 4B, blue

254  box). Quantification of the *Efnb2$^{GFP}$* signal at E18 confirmed a boundary in

255    expression of *Efnb2* in regions of organized cells, but not in adjacent non-organized

256    regions (Figure 4B).

257

258    At P0 *Efnb2* was consistently expressed (and more strongly than at E18) by the line

259    of Prox1$^{hi}$ VFCs and in cells downstream, but not upstream, of the VFCs (Figure 4A,

260    lower panel). Quantification confirmed the boundary in *Efnb2$^{GFP}$* signal, with a peak

261    in *Efnb2* expression coinciding with Prox1$^{hi}$ VFCs (Figure 4C). Whilst at E18 the

262    downstream *Efnb2$^{GFP}$* signal was marginally higher than the upstream signal (Figure

263    4A,B), by P0 this difference was more marked (Figure 4A,C). These results suggest

264    that the *Efnb2* expression boundary is formed concomitantly with the organization of

265    Prox1$^{hi}$ VFCs, and suggest that an Eph-ephrin interaction within venous endothelia

266    might participate in the regulation of VFC organization.

267

268    Analysis of this valve-forming region at P0 in wildtype mice by transmission electron

269    microscopy (TEM) demonstrated that development of the core of the valve leaflet is

270    more advanced than previously characterised, with the presence of interstitial cells

271    within the leaflet, which is already protruding from the vessel wall (Figure 4D, upper

272    panel).(11) VFCs at the leading edge of the protruding leaflet were partly detached

273    from the underlying basement membrane, consistent with their progressive

274    reorientation and migration (Figure 4D, upper panel, arrowheads), as has previously

275    been identified in developing LV.(48) TEM analysis at P6 and in adult mice confirmed

276    the presence of interstitial cells in murine VV (Figure 4D, middle and lower panels,

277    Supplementary Figure 3A-C), consistent with their known presence in, for example,

278    rabbit VV.(2) The presence of interstitial cells in human VV was confirmed by TEM

279    and histology (Supplementary Figure 3D,E). Connexin43 and Connexin47, proteins

280  implicated in human VV disease,(11) were immunolocalised to human VV interstitial

281  cells (Supplementary Figure 3F).

**282  *Efnb2 is required for normal VFC organization***

283  Having established the expression pattern of *Efnb2* during VFC organization, we then

284  examined whether *Efnb2* is required for the organization of VFCs at P0. We

285  performed conditional gene deletion using floxed *Efnb2* alleles and *Prox1Cre^ERT2^,*

286  and quantified each valve according to developmental stage and also quantified the

287  elongation and reorientation of Prox1^hi^ cells (as previously described).(11, 12, 48)

288  Heterozygous deletion at E15 did not significantly affect VV development to stage 1

289  (Figure 5A middle panel, and B). There was, however, a small but significant

290  reduction in VFC nuclear elongation (Figure 5C,D), but no difference in their

291  reorientation (Figure 5E,F). Homozygous deletion of *Efnb2* resulted in disorganized

292  VFCs that failed to reach stage 1 of development at P0, with a similar pattern of

293  disorganization to that seen with deletion of *Ephb4* (P<0.001, Figure 5A lower panel,

294  and B). Prox1^hi^ cells were present but appeared to be distributed across a wider

295  upstream-downstream region of the vessel, and exhibited markedly reduced

296  elongation (Figure 5C,D, P<0.00005) and reorientation (P<0.005, Figure 5E-F).

297  These findings demonstrate that endothelial *Efnb2* is required for the normal

298  organized patterning of VFCs at P0.

299

300  These results, together with those we described for *Ephb4*, show that the expression

301  of EphB4 and *Efnb2* is dynamic during VV organization, and complementary

302  expression (*Efnb2* higher downstream, EphB4 higher upstream) occurs during the

303  process of organization at E18, but by P0 VFCs express both *Efnb2* and EphB4.

304

305

**_Efnb2 is required for projection of VFCs into the vessel lumen, normal_**
**_expression of_ integrin-α9, and normal polarity**

308

We prepared longitudinal semi-thin sections in the XZ-plane of the wholemount
preparations, to more clearly examine projection of VFCs into the vessel lumen.
Compared with littermate controls VFCs failed to project into the vessel lumen in
homozygous _Efnb2_-deleted cells (Figure 6A,B). We hypothesised that failure to
correctly express integrin-α9 could be a mechanism underlying the failure of VFCs to
organize and project into the lumen in _Efnb2_-deleted mice, as integrin-α9 is required
in valve formation for extracellular matrix remodeling, and for VV leaflet growth and
maintenance.(11, 12, 49) At P0 integrin-α9 expression was largely localised to the
line of VFCs on the anterior vein wall (Figure 6C, upper panel). After _Efnb2_ deletion,
the integrin-α9 expression pattern followed the abnormal, broader distribution of the
Prox1^{hi} cells, and appeared haphazard (Figure 6C), likely precluding normal matrix
remodeling.

321

Because VFCs appeared in a broader region after _Efnb2_ deletion, we hypothesised
that without guidance from ephrin-Eph interactions at E18 these cells would be
disorientated at P0. In LV formation, lymphatic ECs elongate and migrate centrally
from the edges of the vessel (48, 50) and in migratory ECs, the Golgi apparatus is
positioned apically of the nucleus.(51) We therefore analysed VFC alignment by co-
staining for a Golgi marker, and examined the alignment of cells with the forming VV
structure (Figure 6D, upper panel). In littermate controls at P0, cells were consistently

329    aligned across the vessel anterior wall, whilst in all samples with homozygous *Efnb2*

330    deletion there was a disrupted pattern (Figure 6D, lower panel).

331    ***Gap junction intercellular communication and proliferation***

332    Expression of ephrinB's may regulate cell behaviour by modulating connexin

333    communication domains, including via Connexin43 (Cx43).(32, 46) Cx43 and

334    Connexin37 (Cx37) have highly regulated expression patterns around VFCs at P0,

335    and both are required for venous, lymphatic, and lymphovenous valve formation.(11,

336    13, 14, 52-54) Large gap junction plaques containing Cx37 are normally expressed

337    by Prox1$^{hi}$ VFCs at P0, whilst Cx43 is primarily expressed in a region just upstream

338    of the organized VFCs at P0. Homozygous deletion of Cx43 (using Prox1Cre$^{ERT2}$), or

339    homozygous knockout of Cx37, results in a failure of organization of VFCs at P0,

340    which is reminiscent of the phenotype seen with homozygous deletion of *Efnb2*.(11,

341    13, 14) This failure of organization at P0 is followed by complete loss of valve

342    structure.(13) We therefore examined the expression patterns of Cx37 and Cx43

343    relative to *Efnb2* expression in the *Efnb2$^{GFP}$* reporter mice, and after homozygous

344    deletion of *Efnb2.* The normally highly restricted expression patterns of Cx37 and

345    Cx43 were disrupted at P0 following homozygous *Efnb2* deletion (Figure 7A,B). In

346    the *Efnb2$^{GFP}$* reporter, Cx37 localisation indicated gap junction plaque formation

347    around *Efnb2*-expressing VFCs (Figure 7A, white arrowheads in upper panel), whilst

348    after *Efnb2* deletion, no plaque formation was identified (or possibly plaques were

349    very much smaller), and Cx37 expression appeared more widespread in the region of

350    the VFCs (Figure 7B).

351

352    In previous genetic loss-of-function experiments (including knockout of Cx37),

353    disruption of VFC organization was associated with a reduction in VFC

354     proliferation,(11) and so we next examined whether deletion of *Efnb2* altered VFC

355     proliferation or apoptosis. As previously, Ki67-positive proliferating VFCs appeared

356     more abundant in the superior & inferior regions of the valve at P0.(11) A reduction in

357     the proportion of proliferating VFCs was seen following *Efnb2* deletion ($P<0.001$,

358     Figure 7C,D), but no effect on apoptosis (as detected by Caspase-3 expression) was

359     observed (data not shown).

360

**Discussion**

We have identified human venous valve failure and deep venous reflux caused by mutations in *EPHB4*. This phenotype was more severe (i.e. a greater loss of valves) than that previously identified in patients with mutations in *FOXC2* or *GJC2* (a fold change vs controls of 0.2 ±SD 0.29 (mosaic *EPHB4*) or 0.17 ±0.36 (constitutive heterozygous *EPHB4*) for the reduction in mean VVs per vein).(11) Almost all of these patients did not have clinical evidence of chronic lower limb primary lymphedema. Some presented with non-immune foetal hydrops, which was of lymphatic origin, but it had resolved soon after birth. Following that, their most obvious clinical sign of disease was early onset prominent or varicose veins, and venous insufficiency.(21) We now know that this is venous valvular aplasia, and therefore mutations in *EPHB4* should be considered as a cause of primary venous valvular aplasia.(5-8, 21, 55) Dysfunction of the deep venous valves increases the rate of progression of chronic venous insufficiency, with a higher rate of chronic venous ulcer formation. The management of deep venous reflux is extremely challenging, as currently there are no reliably effective therapies beyond invasive surgical construction of neovalves.(3)

Heterozygous mutations in *EPHB4* are reported to cause CM-AVM2, vein of Galen aneurysmal malformation, Lymphatic Related Foetal Hydrops (LRFH), and central conducting lymphatic anomaly (CCLA), but the mechanism(s) underlying these different presentations remain unclear.(21, 22, 25, 26, 28) The clinical descriptions of patients with a lymphatic phenotype such as LRFH and CCLA also include clear features of venous disease such as varicose veins, venous hypertension or venous

386    reflux. Similar to the cases presented, it seems likely that the patients reported by Li

387    *et al* may also be affected by VV aplasia and deep venous reflux (considering their

388    increased lower limb pigmentation and venous stasis).(25) The early age at onset of

389    clinical signs of venous insufficiency (for example varicose veins, hemosiderin

390    deposition) in affected individuals, and the near absence of VVs in the scanned veins

391    of affected children observed here, is consistent with a failure of VV formation, rather

392    than early degeneration. These features are not described for CM-AVM2, or vein of

393    Galen aneurysmal malformation, and it is unclear whether the mutations causing

394    these syndromes will also cause VV defects.(22, 26) EphrinB2 is required for normal

395    cardiac valve (CV) formation in mice, but no CV defects were noted on

396    echocardiography in the patients reported here, or those reported elsewhere.(21, 25,

397    28) It remains unclear how, in the settings of developmental blood vessel formation

398    and in the adult capillary bed, ephrinB2-EphB4 interaction leads to specification and

399    subsequent maintenance of arterial and venous endothelia, yet both are expressed in

400    mature veins to regulate the formation of valves.(12, 22, 23, 38, 41) Further work is

401    needed to delineate the context and maturation-dependent regulation of these

402    endothelia.

403

404    Previous *in-vitro* analysis of the *EPHB4* mutations studied here (p.Arg739Glu and

405    p.Ile782Ser) demonstrated that they exhibit greatly reduced kinase activity, but do

406    not exert a dominant negative effect on the expression of wildtype EPHB4

407    protein.(21) Any effect on wildtype EPHB4 activity is unknown. The ratio of ephrinB2

408    to EphB4 expression is disturbed at both mRNA and protein level in ECs cultured

409    from patient arterio-venous malformations, with greatly reduced EphB4 expression

410    compared to a control cell line.(56) The mutant EPHB4 protein implicated in CM-

411   AVM2 becomes trapped in vesicles (22, 28), whilst that implicated in LRFH is

412   presented on the cell membrane (28), but the exact signalling implications of these

413   findings are yet to be elucidated. The requirement for ephrin-Eph signalling at

414   multiple stages of VV development and maintenance complicates any attempt to

415   develop molecular therapy aiming to directly restore valve function. It is possible that

416   pharmacological stimulation or inhibition of the pathway downstream of EPHB4 might

417   be helpful to overcome the resulting aberrant signalling.(22, 25)

418

419   The extent of overlap of the genetic causes of venous valve failure and varicose

420   veins is unclear since regulation of VVs is understudied, but some important

421   indications of similarity have already emerged, including the identification of *PPP3R1*

422   and *PIEZO1* in genome wide association studies of varicose veins, and in mice as

423   critical regulators of VV development.(11, 57, 58) Delineating the roles of the various

424   genes implicated in VV pathogenesis is important and may lead to novel therapies,

425   which could be targeted towards patients at risk of deterioration to chronic

426   ulceration.(59)

427

428   In this study we have identified a striking 'boundary' in the endothelial expression of

429   *Efnb2* at the site of developing VVs (meaning a demarcation between ephrinB2$^{lo}$

430   upstream cells and ephrinB2$^{hi}$ VFCs and cells immediately downstream), and that

431   both ephrinB2 and EphB4 are required for normal organization of VFCs at this critical

432   stage of development in mice. Since ephrinB2 remains the only known ligand for

433   EphB4, this leads us to speculate that an ephrinB2-EphB4 interaction within venous

434   endothelia regulates VV formation. We also show that EphB4 is required for VV

435   maturation. At E18, in areas where VFCs appeared to be in the process of

436 reorientating to become transversely aligned, EphB4 expression was stronger just

437 upstream of the ephrinB2-expressing VFCs. We speculate that at this time point,

438 EphB4$^{hi}$ regions upstream from VFCs may be acting to repel ephrinB2$^{hi}$ VFCs,

439 guiding them to reorientate to lie transversely across the vessel to form a line across

440 the anterior of the lumen. We were unable to localise ephrinB2 because of a lack of

441 specific antibodies, and this inability to colocalise EphB4 and ephrinB2 is a limitation

442 of our study. In wildtype littermates VFC polarity was aligned with the boundary and

443 developing ring of VFCs, whilst after *Efnb2* deletion VFC polarity was disorganized

444 and cells were spread over a wider upstream-downstream region. These results are

445 consistent with previous *in-vitro* findings, showing that ephrinB2-EphB4 interaction

446 leads to separation and clustering of initially mixed populations of EphB4- and

447 ephrinB2-expressing ECs.(47) *In-vitro,* treatment with ephrinB2-Fc stimulates

448 migration of HUVECS, and it is possible that ephrinB2 promotes the migration of

449 VFCs.(60)

450

451 It remains unknown how *Efnb2* expression within veins is regulated. We have shown

452 that the *Efnb2* boundary forms as the VFCs organize, and it may be regulated by the

453 VFCs themselves as they organize. Notably, BMP9 controls lymphatic remodeling

454 and LV formation, and also induces *Efnb2* expression in lymphatic and blood

455 endothelia in vitro, but it is not known whether there is a VV phenotype in *Bmp9$^{-/-}$*

456 mice.(61, 62) The extent to which there is proliferation of VFCs between E18 and P0,

457 or whether there is de-novo differentiation of new Prox1$^{hi}$ cells from surrounding

458 endothelium, remains unclear.

459

460 Normal blood flow is required for postnatal VV maturation (11) and *Efnb2*-dependent

461 protrusion of cells into the lumen at P0 could expose VFCs to higher fluid shear

462 forces, particularly as the vessel lumen becomes more acutely narrowed (e.g. at

463 stage 2 of VV development).(12) Shear-regulated signaling might co-ordinate

464 subsequent events in VV formation, for example commissure formation. In embryonic

465 stem cell derived ECs in vitro, *Efnb2* is upregulated by shear stress, which may

466 contribute to the stimulation of VV leaflet growth post-natally.(12, 63) This notion is

467 consistent with the role of the oscillatory shear stress/Gata2/Foxc2 axis in LV

468 endothelial differentiation, and the potential role of wall shear stress gradients in

469 demarcating the locations of valve formation upstream of tributaries.(64-66) Deletion

470 of the mechanosensory ion channel *Piezo1* results in defective VVs at P3, again

471 consistent with a role for fluid shear in patterning VV (in addition to LV) formation.(57,

472 67)

473

474 Signaling downstream of ephrin-Eph interactions can, for example, inhibit gap

475 junction formation at the boundary between two cell populations, likely by cell

476 repulsion preventing stable contacts between cells.(32) It seems likely that cell-cell

477 repulsion between ephrinB2$^{hi}$ VFCs and EphB4$^{hi}$;ephrinB2$^{lo}$ upstream cells at E18

478 patterns the migration of VFCs. It is unknown whether gap-junction signalling is

479 important in this process, but loss of either Cx37 or Cx43 in mice leads to a similar

480 phenotype with failure of VFC organization.(11) Homozygous *Efnb2* deletion

481 disrupted the normally highly restricted expression patterns of Cx37 and Cx43 at P0,

482 suggesting that gap junctional communication is disrupted. Gap junction plaque size

483 varies depending on how many channels are clustered in the plaque. It is possible

484 that plaques were present but much smaller, although this would also be expected to

485 reduce cell-cell communication.(68) We were unfortunately unable to develop

486 experiments to demonstrate gap junctional VFC cell-cell communication in vivo, or

487 confirm how this may be disrupted after deletion of *Ephb4* or *Efnb2*.

488

489 Mutations in *EFNB1* cause craniofrontonasal syndrome, whilst mice heterozygous for

490 *Efnb1* display skull defects that are thought to be mediated by inhibition of normal

491 gap-junctional communication via Cx43 at ectopic ephrin-Eph boundaries. EphrinB1

492 directly interacts with Cx43 and regulates its cellular distribution, and disruption of

493 gap junction plaques was seen in *Efnb1*^{+/-} mice.(46) Whilst deletion of *Efnb2* resulted

494 in loss of large Cx37 plaques in VFCs, any direct interaction between ephrinB2 and

495 Cx37 remains to be determined. Although not directly demonstrated in our

496 experiments, it is reasonable to assume that following *Efnb2* deletion, as the Prox1^{hi}

497 VFCs are further apart and are physically separated, there will be less

498 communication between these cells via gap junctions (e.g. incorporating Cx37).

499 EphrinB2 organizes VFC positioning and therefore facilitates the formation of

500 functional gap junctions between adjacent VFCs. It is plausible, therefore, that

501 disruption of connexin expression patterning and gap junctional communication may

502 be part of the mechanism that underlies the phenotype seen following *Efnb2*

503 deletion.(46)

504

505 In wildtype mice at P0 Cx43 was expressed upstream of the developing VV and was

506 not clearly expressed by the Prox1^{hi} VFCs that express ephrinB2.(11) Cx43 is clearly

507 expressed by cells that also express EphB4. With deletion of *Efnb2,* Cx43 expression

508 appeared more dispersed throughout the femoral vein, suggesting ephrinB2 is

509 required for the restriction of the Cx43 expression domain. In cardiomyocytes, EphB4

510    physically associates with Cx43, and EphB activation inhibited cardiomyocyte gap

511    junctional electrical coupling.(69) It is possible that in upstream endothelia, signaling

512    through EphB4 could inhibit gap junction communication via Cx43.

513

514    It is unclear why the VV phenotype following *Ephb4* deletion was slightly weaker than

515    that in *Efnb2* deleted mice. EphrinB2 is more promiscuous, binding to EphB4, EphB3

516    and EphB2, while EphB4 exclusively interacts with ephrinB2.(38, 70) Isolated

517    knockout of either *Ephb2* or *Ephb3* does not induce any cardiovascular phenotype,

518    but a third of double knockouts have severely defective angiogenesis that resembles

519    much of the phenotype of *Efnb2*$^{-/-}$ mice.(38) EphB3 expression has been reported in

520    veins (while EphB2 is expressed in nonvascular mesenchymal cells), but we could

521    not detect specific signals for EphB2 or EphB3 in veins by immunohistology (data not

522    shown). EphrinB2 regulates cell morphology and motility independently of binding its

523    receptors in vitro, which could partly explain the stronger phenotype seen with *Efnb2*

524    deletion.(71) In sprouting angiogenesis, ephrinB2 is required for endocytosis and

525    signalling of other important regulators of EC function including Vegfr2 and Vegfr3

526    (which are expressed in developing VVs), and could play similar roles in VFC

527    organization.(12, 39, 40)   The slight difference in the phenotypes following deletion

528    of *Efnb2* and *Ephb4* could be caused by differences in their protein stability, which

529    we were unable to investigate, in part because of the lack of specific antibodies

530    raised against ephrinB2. We could not confirm reduced *Ephb4* or *Efnb2* mRNA levels

531    following conditional gene deletion, due to our inability to specifically isolate venous

532    valve cells, but this has been confirmed for *Efnb2* deletion in lymphatic

533    endothelium.(72)

534

535 Detachment of VFCs from their underlying basement membrane has previously been

536 identified in LV formation, during angiogenesis, and we now show it here in VV

537 formation.(48, 73) Due to detachment, cell-cell contacts are highly restricted, and this

538 is likely to impact cell-cell signalling processes.(48, 74) In vitro, soluble ephrinB2-Fc

539 acts anti-adhesively, and the high ephrinB2 expression in VFCs could promote their

540 detachment from the underlying basement membrane to facilitate reorientation and

541 organization.(47)

542

543 We have previously analysed VFC nuclear reorientation and elongation in

544 wholemount confocal microscopy to characterise phenotypes at P0 / stage 1 of VV

545 development.(11) Here, we show that VFCs not only protrude into the vessel lumen

546 at this stage, but that this protrusion is abolished following homozygous *Efnb2*

547 deletion. We also identify that ingress of interstitial cells is already occurring at this

548 early stage and confirm their persistence in P6 and adult murine VV, and in adult

549 human VV. Their existence has previously been demonstrated in human, rat and

550 rabbit VV, in contrast to LV, which lack interstitial cells.(2, 49, 54) In lymphovenous

551 valve development, mural cells are recruited into the valve leaflets during maturation,

552 but the developmental origin of these cells in VVs is currently unknown.(54) The

553 identity, origin and functions of these cells in VVs will be the subject of future studies.

554

555 Our data showing that EphB4 is required for post-natal development is consistent

556 with the phenotype resulting from *Efnb2* deletion at P2 or P0.(11, 12) Almost all

557 Prox1^{hi} and Foxc2^{hi} VFCs were absent at P6, in contrast to deletion of *Ppp3r1*

558 (CnB1) in which a clear ring of Prox1 and Foxc2-expressing cells remains.(11) This is

559 consistent with a requirement for EphB4 (and ephrinB2) to develop/maintain the

560 phenotype of free-edge cells to P6, rather than just growth of VV leaflets.(11) The

561 failure to establish a local reduction in the density of smooth muscle cells (SMCs)

562 around the VV at P6 after *Ephb4* deletion at P0 is consistent with the endothelial

563 VFC-to-SMC signaling that controls this reduction in SMC density around LVs.(31,

564 75-77)


565 **Conclusions**

566

567 In addition to an increased risk of lymphatic-related foetal hydrops, we have shown

568 that patients carrying heterozygous mutations in *EPHB4* have very few VVs, with

569 early onset deep venous reflux indicating that the observed venous insufficiency is

570 due to venous valve aplasia.  By studying mice, it was demonstrated that ephrinB2

571 and EphB4 pattern the organization of valve-forming cells at P0, and are required for

572 cellular reorientation, elongation, protrusion and proliferation, adding to our

573 understanding of the complex venous valve developmental programme. Postnatal

574 deletion of *Ephb4* leads to complete loss of the valve, which could explain the

575 phenotype observed in the patients.

576

577

## Methods

### Human VV ultrasonography

The brachial, basilic, popliteal, and short saphenous veins underwent ultrasonographic evaluation in London (Phillips IU22 with L17-5MHz/L9-3MHz probes) and VV maximum leaflet measurements obtained offline (Xcelera Cath Lab software, Phillips). Reproducibility was determined previously.[11] For each vein, the number of VVs and VV length was normalised to the mean value in the respective control veins from our existing control population, and additional new controls, and the mean number of VVs per vein, per patient, was compared. Deep venous (popliteal) reflux duration was measured bilaterally after distal manual compression whilst standing, and the mean taken, with reflux defined as ≥0.5s, and severe reflux as >1s.[78-80] Because deep venous reflux is rare, popliteal venous reflux was not routinely measured in the entire control population, but was subsequently measured in additional controls.[81] Genotyping was performed at St George's, University of London and in Bergen.[21]

### Mouse lines

Wildtype analyses were carried out in BALB/C mice obtained from Charles River UK. *Prox1CreER$^{T2}$* (12), Rosa26$^{mTmG}$ (82), *Efnb2$^{lx}$* (83), and *Efnb2$^{GFP}$* (84) mice have been described previously and were maintained on C57BL/6 backgrounds. Tamoxifen/4OH-Tamoxifen (in peanut or sunflower oil, Sigma) was injected i.p. either 1mg at E15 for analysis at P0, or 50µg at P0 for analysis at P6 in order to induce Cre activity in *Prox1CreER$^{T2}$* mice.[12] To delay labour 37.5µg/g.Ms weight progesterone was given i.p. at E15+E18 and embryos analysed at 'E19', equivalent to P0. We

603    compared VV in *Prox1CreER^{T2}*+ with *Prox1CreER^{T2}*- littermate controls in all deletion

604    experiments.

605

606    **Electron microscopy**

607    Mice were culled and perfused via the aorta with heparinised PBS (hPBS, 25mg/L,

608    MP Biomedicals) prior to fixation overnight in glutaraldehyde (2.5% v/v in 0.1M

609    cacodylate buffer, pH 7.4, 4°C) and post-fixation in osmium tetroxide (1% w/v in 0.1M

610    cacodylate, pH 7.4, 4°C) for 1.5hrs. All samples were dehydrated through graded

611    ethanols, equilibrated with propylene oxide, infiltrated with epoxy resin (TAAB) and

612    polymerised at 70°C for 24hrs. Semithin sections (0.45µm) were cut and stained with

613    1% Toluidine Blue. For analysis of protruding VFCs, >90 serial semithin sections

614    were analysed per sample (unpaired t test). For 3D reconstructions at P0, semi-thin

615    sections (0.45µm) were photographed (Leitz DMRB microscope, Micropublisher

616    3.3RTV camera), aligned in ImageJ (NIH) and reconstructed using Amira (Thermo

617    Fisher Scientific). Ultrathin sections (50-70nm, Reichert-Jung ultramicrotome) were

618    mounted and contrasted using uranyl acetate/lead citrate for examination (Hitachi

619    H7600, 80kV, AMT digital camera).[85] For quantification of interstitial cells at P6, the

620    length of the leaflet was measured in ImageJ, and the number of whole interstitial cell

621    nuclei counted. Human great saphenous veins (obtained during coronary artery

622    bypass grafting) were opened prior to processing as per murine samples, with

623    visualisation of ultrathin sections using a Hitachi S-3500N microscope.

624

625    **Immunohistochemistry**

626    Mice were culled and perfusion fixed via the aorta and femoral vein by perfusion with

627    hPBS followed by 4% formaldehyde, and then further fixed for 24hrs. The external

628 iliac and femoral veins were excised, embedded in wax, and 5µm sections were

629 incubated with primary antibody and washed prior to amplification using polymer

630 horseradish peroxidase (Menarini) and signal detection using SG peroxidase

631 substrate (Vector). Sections were photographed using a Micropublisher 3.3RTV

632 camera mounted on a Leitz DMRB microscope with PL Fluotar ×20 lens (Leica).

633

634 **Wholemount immunostaining and analysis**

635 Mice were culled and perfused with hPBS via the aorta prior to fixation in 4%

636 paraformaldehyde (PFA) followed by blocking in 3%v/v donkey serum, 0.3% Triton-

637 x100 and further dissection prior to incubation with primary antibodies, and washing

638 prior to localisation with fluorophore-conjugated secondary antibodies. Samples were

639 finally dissected and mounted in Prolong Gold (Invitrogen). Valves were imaged

640 using a Leica SP5 confocal microscope (1024x1024 resolution, 8-bit) to produce Z

641 projections (NIH ImageJ) of median filtered (Leica LASAF/ImageJ, except for

642 connexin localisation or fluorescence quantification) stacks. Lookup tables were

643 linear. Control samples were incubated either with the appropriate non-immune IgG

644 and then secondary antibody, or streptavidin-conjugated fluorophore alone

645 (Supplementary Figure 2A).

646

647 For analysis of VFC organization, Prox1^{hi} nuclear elongation (proportion with

648 length:width ratio ≥2) and reorientation (proportion with long axis ≥40degrees from

649 the vessel centreline, in nuclei with length:width ratio ≥2) were quantified in z-

650 projections (NIH ImageJ) as previously described.(11, 48)

651

652    For analysis of *Efnb2^GFP* expression at E18-P0 (Figure 4) Z-projections of confocal z-

653    stacks were oriented with flow left to right and the centre line of the vessel horizontal.

654    For each valve 7-12 10x100µm regions of interest, each centred on the VFC

655    upstream edge, were analysed (ImageJ). Mean intensity profiles for each fluorophore

656    were converted to z-scores and the mean of 6 VVs plotted. At E18, areas with and

657    without Prox1$^{hi}$ organizing VFCs were analysed separately.

658    For analysis of areas of expression of Ephb4 and Efnb2GFP at E18 (Figure 2B) an

659    XZ projection (13.6µm deep) across the reorientating VFCs was reconstructed (NIH

660    ImageJ) and the relative fluorescence intensity profile for Efnb2GFP and EphB4

661    plotted. For quantification, for each valve 4-6 50µm linear regions of interest were

662    drawn, centred on the VFC leading edge, at E18, for N=6 VVs. Ephb4 upstream vs

663    downstream intensity was compared (T Test).

664

665    For analysis of cell orientation by co-immunostaining of nucleus and Golgi, stacks of

666    0.5µm optical sections were analysed (ImageJ) to identify the Golgi for each VFC,

667    and an arrow drawn from nuclear centre to Golgi centre. The z-projection of all

668    arrows is shown.

669

670    **Antibodies**

671    Antibodies: Rabbit anti- Cx43 (Cell Signaling Technology 3512), Cx37 (CX37A11,

672    Alpha diagnostics), Prox1 (11-002P, Angiobio), ki67 (ab15580, Abcam), and Golgi

673    apparatus protein 1 (ab103439, Abcam); sheep anti- Foxc2 (AF6989, R&D); goat

674    anti- EphB4 (BAF446, R&D); rat anti- PECAM1 (clone MEC 13.3, BD); and mouse

675    anti- $\alpha$ smooth muscle actin (clone 1A4 conjugated to Cy3, Sigma). For fluorescence

676 signal detection secondary antibodies or streptavidin were conjugated to Dylight-

677 405/488/550/649 (Jackson Immunoresearch).

678

679 **Statistics**

680 For VV developmental stage 0-4 quantification, data represent the proportion of VV

681 reaching each developmental stage. P values represent the difference in proportion

682 of valves at each stage versus their wild-type littermates (Chi square/Fisher's Exact

683 test as appropriate). Comparisons of VFC nuclear elongation and reorientation

684 between groups were analysed by one-way ANOVA & Bonferroni post hoc tests. Age

685 and sex matching for patient ultrasonography was tested respectively by two-tailed

686 unpaired t-test and Fisher's exact test. All analyses were carried out using IBM SPSS

687 Statistics 24, and Graphpad PRISM v8. A P value less than 0.05 was considered

688 significant. Ultrasonographers were blinded to participant genotype during scanning,

689 and image analysis/quantification. Experiments were not randomised.

690

691 **Study approval**

692 All human studies and animal studies were carried out in accordance with national

693 regulations and ethical approvals in the UK and Sweden (Health Research Authority

694 12/LO/1164, 10/H0701/68, C130/15). Written informed consent was obtained from all

695 participants.

696

697 **Author contributions**

698 The authors have declared that no conflict of interest exists.

699 All authors designed research studies, OL, JW, CS, MI, AA, MH, MF, GV conducted

700 experiments, acquired & analysed data. PM, SJ, SB, SM, PO, provided patients; OL,

708　**Supplemental Data**

709　Supplemental data includes one table and three figures.


710　**References**

711　1.　Phillips MN, et al. Micro-venous valves in the superficial veins of the human

712　　lower limb. *Clin Anat.* 2004;17(1):55-60.

713　2.　Gottlob R, et al. *Venous valves : morphology, function, radiology, surgery.*

714　　Wien ; New York: Springer-Verlag; 1986.

715　3.　Eberhardt RT, and Raffetto JD. Chronic venous insufficiency. *Circulation.*

716　　2014;130(4):333-46.

717　4.　Labropoulos N, et al. The role of venous reflux and calf muscle pump function

718　　in nonthrombotic chronic venous insufficiency. Correlation with severity of

719　　signs and symptoms. *Arch Surg.* 1996;131(4):403-6.

720　5.　Friedman EI, et al. Congenital venous valvular aplasia of the lower extremities.

721　　*Surgery.* 1988;103(1):24-6.

722  6.  Gorenstein A, et al. Congenital aplasia of the deep veins of lower extremities

723      in children: the role of ascending functional phlebography. *Surgery.*

724      1986;99(4):414-20.

725  7.  Bollinger A, et al. [Valve agenesis and dysplasia of leg veins. Morphological

726      and functional studies]. *Schweizerische medizinische Wochenschrift.*

727      1971;101(37):1348-53.

728  8.  Plate G, et al. Congenital vein valve aplasia. *World J Surg.* 1986;10(6):929-34.

729  9.  Meissner M, et al. The hemodynamics and diagnosis of venous disease.

730      *Journal of Vascular Surgery.* 2007;46(6):S4-S24.

731  10. Lyons OT, et al. Redox dysregulation in the pathogenesis of chronic venous

732      ulceration. *Free radical biology & medicine.* 2019.

733  11. Lyons O, et al. Human venous valve disease caused by mutations in FOXC2

734      and GJC2. *The Journal of experimental medicine.* 2017;214:2437-52.

735  12. Bazigou E, et al. Genes regulating lymphangiogenesis control venous valve

736      formation and maintenance in mice. *J Clin Invest.* 2011;121(8):2984-92.

737  13. Munger SJ, et al. Absence of venous valves in mice lacking Connexin37. *Dev

738      Biol.* 2013;373(2):338-48.

739  14. Munger SJ, et al. Segregated Foxc2, NFATc1 and Connexin expression at

740      normal developing venous valves, and Connexin-specific differences in the

741      valve phenotypes of Cx37, Cx43, and Cx47 knockout mice. *Dev Biol.*

742      2016;412(2):173-90.

743  15.  Goel RR, et al. Surgery for deep venous incompetence. *The Cochrane database of systematic reviews.* 2015(2):CD001097.

745  16.  Geng X, et al. Intraluminal valves: development, function and disease. *Disease models & mechanisms.* 2017;10(11):1273-87.

747  17.  Connell FC, et al. The classification and diagnostic algorithm for primary lymphatic dysplasia: an update from 2010 to include molecular findings. *Clin Genet.* 2013;84(4):303-14.

750  18.  Rosbotham JL, et al. Distichiasis-lymphoedema: clinical features, venous function and lymphoscintigraphy. *The British journal of dermatology.* 2000;142(1):148-52.

753  19.  Mellor RH, et al. Mutations in FOXC2 Are Strongly Associated With Primary Valve Failure in Veins of the Lower Limb. *Circulation.* 2007;115(14):1912-20.

755  20.  Ostergaard P, et al. Rapid identification of mutations in GJC2 in primary lymphoedema using whole exome sequencing combined with linkage analysis with delineation of the phenotype. *J Med Genet.* 2011;48(4):251-5.

758  21.  Martin-Almedina S, et al. EPHB4 kinase-inactivating mutations cause autosomal dominant lymphatic-related hydrops fetalis. *J Clin Invest.* 2016;126(8):3080-8.

761  22.  Amyere M, et al. Germline Loss-of-Function Mutations in EPHB4 Cause a Second Form of Capillary Malformation-Arteriovenous Malformation (CM-AVM2) Deregulating RAS-MAPK Signaling. *Circulation.* 2017;136(11):1037-48.

765    23.   Wooderchak-Donahue WL, et al. Phenotype of CM-AVM2 caused by variants
766          in EPHB4: how much overlap with hereditary hemorrhagic telangiectasia
767          (HHT)? *Genetics in medicine : official journal of the American College of*
768          *Medical Genetics.* 2019;21(9):2007-14.

769    24.   Yu J, et al. EPHB4 Mutation Implicated in Capillary Malformation-
770          Arteriovenous Malformation Syndrome: A Case Report. *Pediatric dermatology.*
771          2017;34(5):e227-e30.

772    25.   Li D, et al. Pathogenic variant in EPHB4 results in central conducting
773          lymphatic anomaly. *Hum Mol Genet.* 2018;27(18):3233-45.

774    26.   Vivanti A, et al. Loss of function mutations in EPHB4 are responsible for vein
775          of Galen aneurysmal malformation. *Brain : a journal of neurology.*
776          2018;141(4):979-88.

777    27.   Duran D, et al. Mutations in Chromatin Modifier and Ephrin Signaling Genes in
778          Vein of Galen Malformation. *Neuron.* 2019;101(3):429-43 e4.

779    28.   Martin-Almedina S, et al. Janus-faced EPHB4-associated disorders: novel
780          pathogenic variants and unreported intrafamilial overlapping phenotypes.
781          *Genetics in medicine : official journal of the American College of Medical*
782          *Genetics.* 2021.

783    29.   Luxan G, et al. Endothelial EphB4 maintains vascular integrity and transport
784          function in adult heart. *eLife.* 2019;8.

785    30.   Hirai H, et al. A novel putative tyrosine kinase receptor encoded by the eph
786          gene. *Science.* 1987;238(4834):1717-20.

787   31.   Kania A, and Klein R. Mechanisms of ephrin-Eph signalling in development,
788          physiology and disease. *Nature reviews Molecular cell biology.*
789          2016;17(4):240-56.

790   32.   Mellitzer G, et al. Eph receptors and ephrins restrict cell intermingling and
791          communication. *Nature.* 1999;400(6739):77-81.

792   33.   Xu Q, et al. In vivo cell sorting in complementary segmental domains mediated
793          by Eph receptors and ephrins. *Nature.* 1999;399(6733):267-71.

794   34.   Batlle E, and Wilkinson DG. Molecular mechanisms of cell segregation and
795          boundary formation in development and tumorigenesis. *Cold Spring Harbor*
796          *perspectives in biology.* 2012;4(1):a008227.

797   35.   Gerety SS, et al. Symmetrical mutant phenotypes of the receptor EphB4 and
798          its specific transmembrane ligand ephrin-B2 in cardiovascular development.
799          *Mol Cell.* 1999;4(3):403-14.

800   36.   Gale NW, et al. Ephrin-B2 selectively marks arterial vessels and
801          neovascularization sites in the adult, with expression in both endothelial and
802          smooth-muscle cells. *Dev Biol.* 2001;230(2):151-60.

803   37.   Shin D, et al. Expression of ephrinB2 identifies a stable genetic difference
804          between arterial and venous vascular smooth muscle as well as endothelial
805          cells, and marks subsets of microvessels at sites of adult neovascularization.
806          *Dev Biol.* 2001;230(2):139-50.

807   38.   Adams RH, et al. Roles of ephrinB ligands and EphB receptors in
808          cardiovascular development: demarcation of arterial/venous domains,

809      vascular morphogenesis, and sprouting angiogenesis. *Genes Dev.*
810      1999;13(3):295-306.

811 39. Wang Y, et al. Ephrin-B2 controls VEGF-induced angiogenesis and
812      lymphangiogenesis. *Nature.* 2010;465(7297):483-6.

813 40. Sawamiphak S, et al. Ephrin-B2 regulates VEGFR2 function in developmental
814      and tumour angiogenesis. *Nature.* 2010;465(7297):487-91.

815 41. Oike Y, et al. Regulation of vasculogenesis and angiogenesis by EphB/ephrin-
816      B2 signaling between endothelial cells and surrounding mesenchymal cells.
817      *Blood.* 2002;100(4):1326-33.

818 42. Makinen T. PDZ interaction site in ephrinB2 is required for the remodeling of
819      lymphatic vasculature. *Genes & Development.* 2005;19(3):397-410.

820 43. Zhang G, et al. EphB4 forward signalling regulates lymphatic valve
821      development. *Nat Commun.* 2015;6:6625.

822 44. Katsuta H, et al. EphrinB2-EphB4 signals regulate formation and maintenance
823      of funnel-shaped valves in corneal lymphatic capillaries. *Investigative*
824      *ophthalmology & visual science.* 2013;54(6):4102-8.

825 45. Cowan CA, et al. Ephrin-B2 reverse signaling is required for axon pathfinding
826      and cardiac valve formation but not early vascular development.
827      *Developmental Biology.* 2004;271(2):263-71.

828 46. Davy A, et al. Inhibition of gap junction communication at ectopic Eph/ephrin
829      boundaries underlies craniofrontonasal syndrome. *PLoS Biol.*
830      2006;4(10):e315.

831    47.    Fuller T, et al. Forward EphB4 signaling in endothelial cells controls cellular

832          repulsion and segregation from ephrinB2 positive cells. *J Cell Sci.* 2003;116(Pt

833          12):2461-70.

834    48.    Tatin F, et al. Planar Cell Polarity Protein Celsr1 Regulates Endothelial

835          Adherens Junctions and Directed Cell Rearrangements during Valve

836          Morphogenesis. *Dev Cell.* 2013;26(1):31-44.

837    49.    Bazigou E, et al. Integrin-α9 Is Required for Fibronectin Matrix Assembly

838          during Lymphatic Valve Morphogenesis. *Developmental Cell.* 2009;17(2):175-

839          86.

840    50.    Bazigou E, et al. Primary and secondary lymphatic valve development:

841          molecular, functional and mechanical insights. *Microvascular research.*

842          2014;96:38-45.

843    51.    Francis R, et al. Connexin43 modulates cell polarity and directional cell

844          migration by regulating microtubule dynamics. *PLoS One.* 2011;6(10):e26379.

845    52.    Kanady JD, et al. Connexin37 and Connexin43 deficiencies in mice disrupt

846          lymphatic valve development and result in lymphatic disorders including

847          lymphedema and chylothorax. *Dev Biol.* 2011;354(2):253-66.

848    53.    Kanady JD, et al. Combining Foxc2 and Connexin37 deletions in mice leads to

849          severe defects in lymphatic vascular growth and remodeling. *Dev Biol.*

850          2015;405(1):33-46.

851    54.    Geng X, et al. Multiple mouse models of primary lymphedema exhibit distinct

852          defects in lymphovenous valve development. *Dev Biol.* 2016;409(1):218-33.

853    55.    Leu HJ. Familiar congenital absence of valves in the deep leg veins.

854          *Humangenetik.* 1974;22(4):347-9.

855    56.    Fehnel KP, et al. Dysregulation of the EphrinB2-EphB4 ratio in pediatric

856          cerebral arteriovenous malformations is associated with endothelial cell

857          dysfunction in vitro and functions as a novel noninvasive biomarker in patients.

858          *Experimental & molecular medicine.* 2020;52(4):658-71.

859    57.    Nonomura K, et al. Mechanically activated ion channel PIEZO1 is required for

860          lymphatic valve formation. *Proc Natl Acad Sci U S A.* 2018;115(50):12817-22.

861    58.    Shadrina AS, et al. Varicose veins of lower extremities: Insights from the first

862          large-scale genetic study. *PLoS genetics.* 2019;15(4):e1008110.

863    59.    Jones GT, et al. A variant of the castor zinc finger 1 (CASZ1) gene is

864          differentially associated with the clinical classification of chronic venous

865          disease. *Scientific reports.* 2019;9(1):14011.

866    60.    Zheng LC, et al. Ephrin-B2/Fc promotes proliferation and migration, and

867          suppresses apoptosis in human umbilical vein endothelial cells. *Oncotarget.*

868          2017;8(25):41348-63.

869    61.    Kim JH, et al. BMP9 induces EphrinB2 expression in endothelial cells through

870          an Alk1-BMPRII/ActRII-ID1/ID3-dependent pathway: implications for

871          hereditary hemorrhagic telangiectasia type II. *Angiogenesis.* 2012;15(3):497-

872          509.

873    62.    Levet S, et al. Bone morphogenetic protein 9 (BMP9) controls lymphatic

874          vessel maturation and valve formation. *Blood.* 2013;122(4):598-607.

875   63.   Masumura T, et al. Shear stress increases expression of the arterial

876         endothelial marker ephrinB2 in murine ES cells via the VEGF-Notch signaling

877         pathways. *Arterioscler Thromb Vasc Biol.* 2009;29(12):2125-31.

878   64.   Mahamud MR, et al. GATA2 controls lymphatic endothelial cell junctional

879         integrity and lymphovenous valve morphogenesis through miR-126.

880         *Development.* 2019;146(21).

881   65.   Sabine A, et al. Mechanotransduction, PROX1, and FOXC2 cooperate to

882         control connexin37 and calcineurin during lymphatic-valve formation. *Dev Cell.*

883         2012;22(2):430-45.

884   66.   Michalaki E, et al. Perpendicular alignment of lymphatic endothelial cells in

885         response to spatial gradients in wall shear stress. *Communications biology.*

886         2020;3(1):57.

887   67.   Choi D, et al. Piezo1 incorporates mechanical force signals into the genetic

888         program that governs lymphatic valve development and maintenance. *JCI*

889         *insight.* 2019;4(5).

890   68.   Solan JL, and Lampe PD. Spatio-temporal regulation of connexin43

891         phosphorylation and gap junction dynamics. *Biochimica et biophysica acta*

892         *Biomembranes.* 2018;1860(1):83-90.

893   69.   Ishii M, et al. EphB signaling inhibits gap junctional intercellular

894         communication and synchronized contraction in cultured cardiomyocytes.

895         *Basic research in cardiology.* 2011;106(6):1057-68.

896 70. Sakano S, et al. Characterization of a ligand for receptor protein-tyrosine kinase HTK expressed in immature hematopoietic cells. *Oncogene.* 1996;13(4):813-22.

899 71. Bochenek ML, et al. Ephrin-B2 regulates endothelial cell morphology and motility independently of Eph-receptor binding. *J Cell Sci.* 2010;123(Pt 8):1235-46.

902 72. Frye M, et al. EphrinB2-EphB4 signalling provides Rho-mediated homeostatic control of lymphatic endothelial cell junction integrity. *eLife.* 2020;9.

904 73. Hirschberg RM, et al. Electron microscopy of cultured angiogenic endothelial cells. *Microsc Res Tech.* 2005;67(5):248-59.

906 74. Dong M, et al. Spatiomechanical Modulation of EphB4-Ephrin-B2 Signaling in Neural Stem Cell Differentiation. *Biophysical journal.* 2018;115(5):865-73.

908 75. Jurisic G, et al. An unexpected role of semaphorin3a-neuropilin-1 signaling in lymphatic vessel maturation and valve formation. *Circ Res.* 2012;111(4):426-36.

911 76. Bouvree K, et al. Semaphorin3A, Neuropilin-1, and PlexinA1 are required for lymphatic valve formation. *Circ Res.* 2012;111(4):437-45.

913 77. Petrova TV, et al. Defective valves and abnormal mural cell recruitment underlie lymphatic vascular failure in lymphedema distichiasis. *Nature Medicine.* 2004;10(9):974-81.

916 78. Sarin S, et al. Duplex ultrasonography for assessment of venous valvular function of the lower limb. *Br J Surg.* 1994;81(11):1591-5.

918   79.   Lurie F, et al. Multicenter assessment of venous reflux by duplex ultrasound. *J*

919        *Vasc Surg.* 2012;55(2):437-45.

920   80.   van Bemmelen PS, et al. Quantitative segmental evaluation of venous valvular

921        reflux with duplex ultrasound scanning. *J Vasc Surg.* 1989;10(4):425-31.

922   81.   Maurins U, et al. Distribution and prevalence of reflux in the superficial and

923        deep venous system in the general population--results from the Bonn Vein

924        Study, Germany. *J Vasc Surg.* 2008;48(3):680-7.

925   82.   Muzumdar MD, et al. A global double-fluorescent Cre reporter mouse.

926        *Genesis.* 2007;45(9):593-605.

927   83.   Grunwald IC, et al. Hippocampal plasticity requires postsynaptic ephrinBs.

928        *Nature neuroscience.* 2004;7(1):33-40.

929   84.   Davy A, and Soriano P. Ephrin-B2 forward signaling regulates somite

930        patterning and neural crest cell development. *Dev Biol.* 2007;304(1):182-93.

931   85.   Venable JH, and Coggeshall R. A Simplified Lead Citrate Stain for Use in

932        Electron Microscopy. *J Cell Biol.* 1965;25:407-8.

933

934

935 **Figure 1**



Lyons_Fig 1
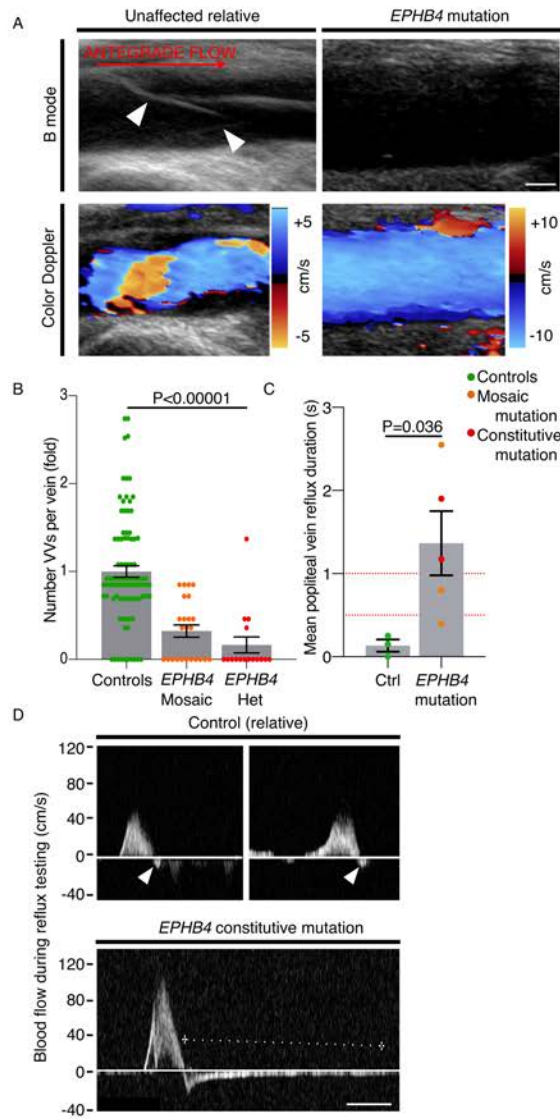
**Figure 1: EPHB4 mutations cause human VV failure**

A) VVs (arrowheads) were readily identifiable in the veins of controls, including an unaffected relative, but were rare in patients with a mutation in *EPHB4*. B-mode and color doppler images are shown of the popliteal vein. Blood flow left to right, velocity indicated by color scale. Bar=2mm

B) Fewer VVs per vein were seen in participants with mosaic or constitutive (heterozygous) *EPHB4* mutation (P=1.7x10-11, ANOVA). N=92 veins in 13 controls, and 40 veins in 5 patients with *EPHB4* mutation (mosaic or constitutive). Data points represent individual veins. Het = heterozygous.

C) Popliteal (deep) venous reflux was identified in mosaic and constitutive carriers of *EPHB4* mutations (P=0.036, Mann-Whitney). Blood velocity ≥0.5s indicates reflux and ≥1s indicates severe reflux (red dotted lines). Data points represent mean of left and right popliteal reflux duration for each individual.

D) Representative blood velocity in the popliteal vein during reflux testing is shown for an unaffected relative (with no significant reflux, arrowheads) and a patient carrying an *EPHB4* mutation, demonstrating significant deep venous reflux (dotted line = 2.14s, bar=500ms). Throughout all figures, antegrade blood flow is from left to right. Error bars indicate SEM.

961 **Figure 2**



Lyons_Fig 2
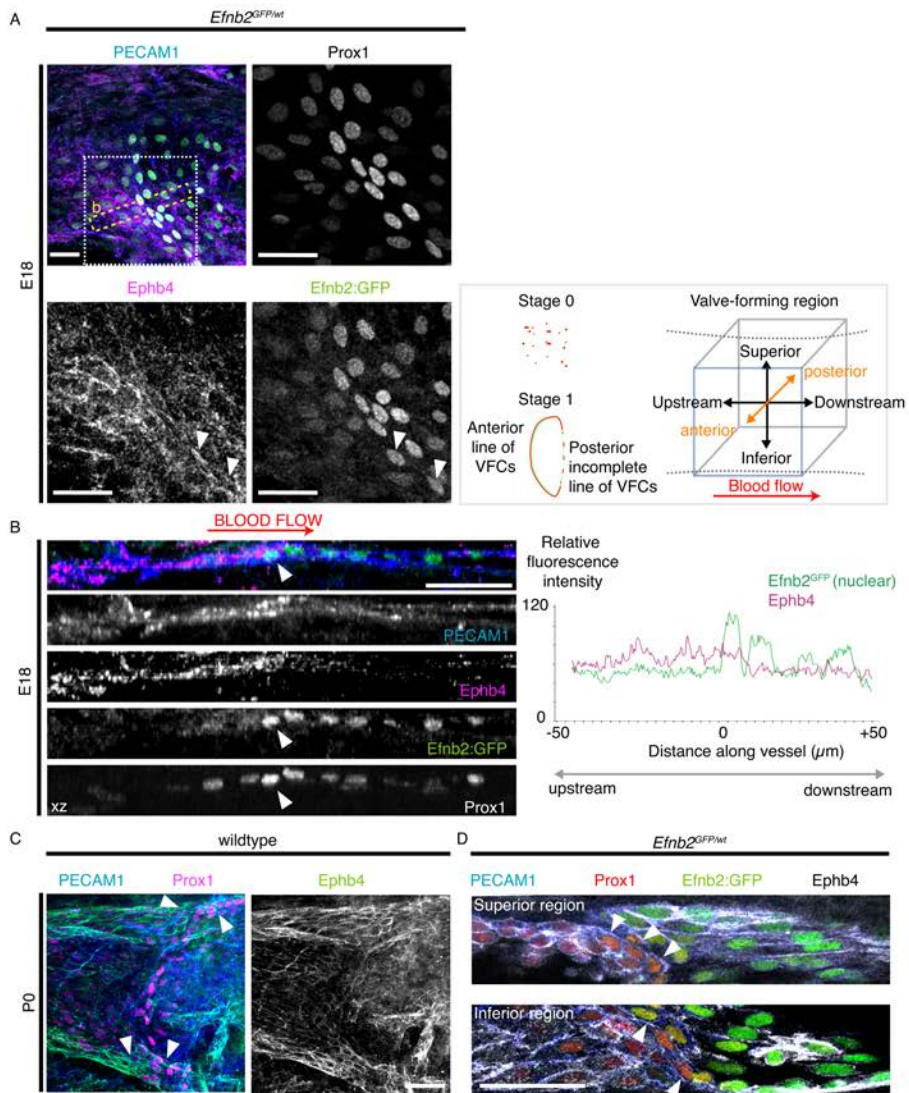
**Figure 2: Expression of EphB4 in Efnb2GFP reporter E18 and P0**

A) Localisation of PECAM1 (blue), Ephb4 (magenta), and Prox1 (white), Efnb2:GFP (green) in heterozygous Efnb2GFP mice at E18. Part of an E18 VV is shown, and the white boxed area (which contains organizing VFCs) is shown enlarged in single channel images. Only the anterior vein wall is shown. Arrowhead indicates a VFC nearer the inferior edge of the vessel co-expressing Ephb4 and Efnb2GFP. The schematic indicates stages 0 and 1 of VV development, as previously defined in Ref 11. Red=Prox1hi VFCs, which form a continuous line across the anterior vein wall at stage 1. The orientation of all confocal z-stacks is indicated and is the same throughout all figures. wt = wildtype.

B) An XZ projection (13.6µm deep), and the fluorescence intensity profile for Efnb2GFP and EphB4 is shown across the organizing VFCs, indicated by the yellow boxed area in A. The EphB4 signal is stronger upstream (to the left) of the VFCs (indicated by arrowheads, or "0" on the graph x axis), whilst the Efnb2GFP signal is stronger in VFCs and downstream. ($P<0.0001$, N=6 VV, T test). The multichannel image does not include Prox1.

C) In wildtype VVs at P0, Prox1hi VFCs expressed EphB4, and it was particularly strongly expressed in the superior and inferior areas of the vein (arrowheads).

D) Co-expression of Ephb4 and Efnb2 was confirmed in *Efnb2GFP* mice. 6µm z-projections of the upper and lower regions of a valve are shown. Arrowheads indicate reorientated VFCs (orange). (Uncropped images are provided in Supplementary Figure 2B). Bars = 20µm
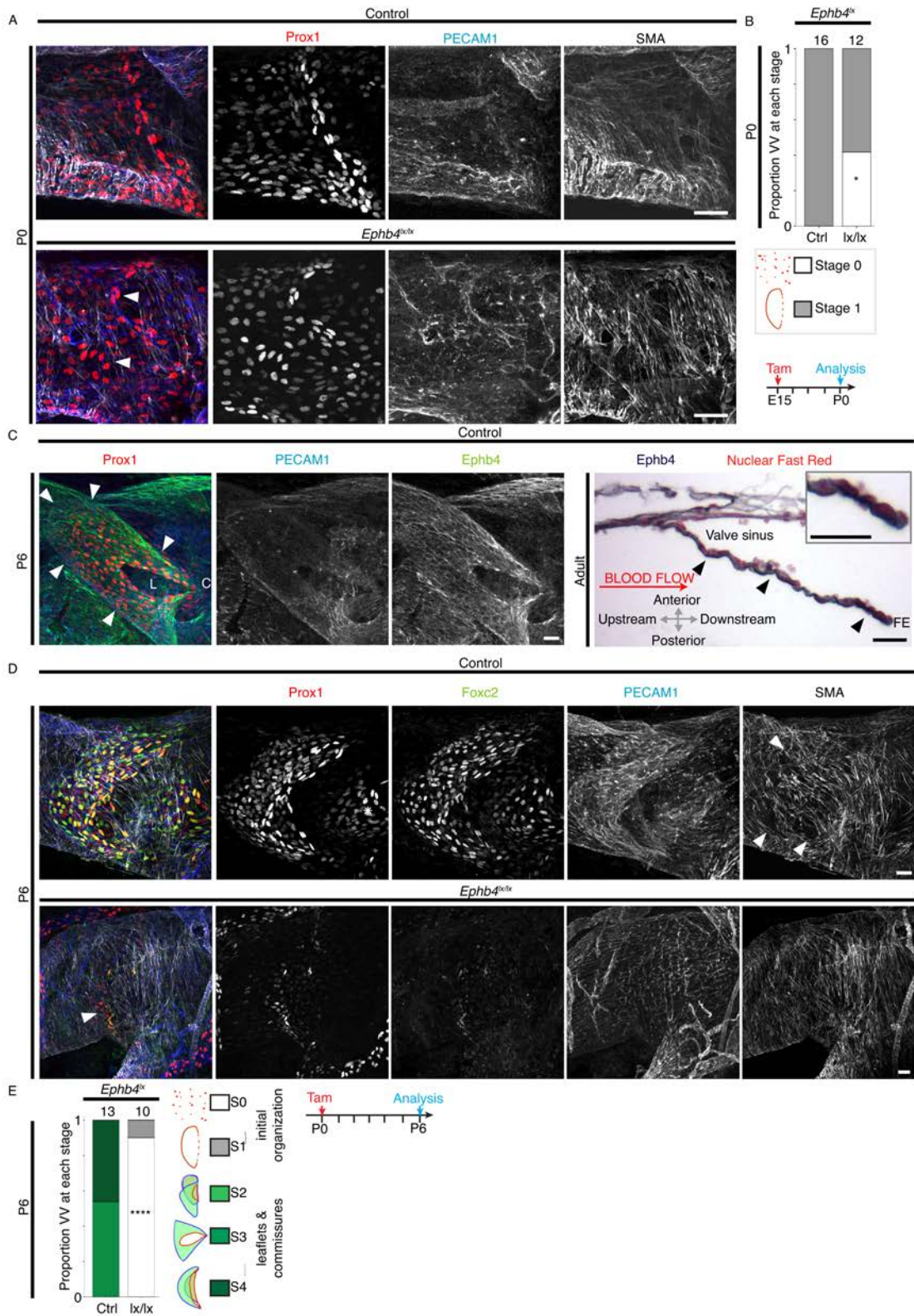
**Figure 3**

**Figure 3: EphB4 is expressed at E18 and P0 and is required for normal VFC organization, and leaflet development to P6**

A-B) Homozygous deletion of *Ephb4* at E15 (analysed at P0) resulted in disrupted organization of VFCs, similar to deletion of *Efnb2*, albeit some VVs appeared to develop normally. The number of VVs analysed for each condition is indicated above each bar in the chart. *=P0.008, Fisher's Exact test. Bars = 20µm. Tam = Tamoxifen, SMA = smooth muscle alpha actin

C) EphB4 was localised in wildtype P6 VVs and surrounding vein. The leaflet of a stage 3 VV is indicated by arrowheads. L=valve lumen and C=the single commissure. In adult VV, longitudinal sections were prepared, and EphB4 (dark blue stain) was most strongly localised to the luminal surface of VV leaflets (black arrowheads) and leaflet free edge (FE, enlarged in inset). The counterstain is Nuclear Fast Red. Arrows indicate the orientation of the adult histological section only (all confocal images are oriented as shown in Fig.2).

D-E) Induction of homozygous *Ephb4* deletion at P0 with Tamoxifen (analysis at P6) resulted in entirely absent VV leaflets, and failure to remodel the surrounding SMCs (arrowheads in upper panel), at P6. Only a few Prox1hi/Foxc2hi cells remained (arrowhead in lower panel). ∗ indicates a downstream tributary valve.
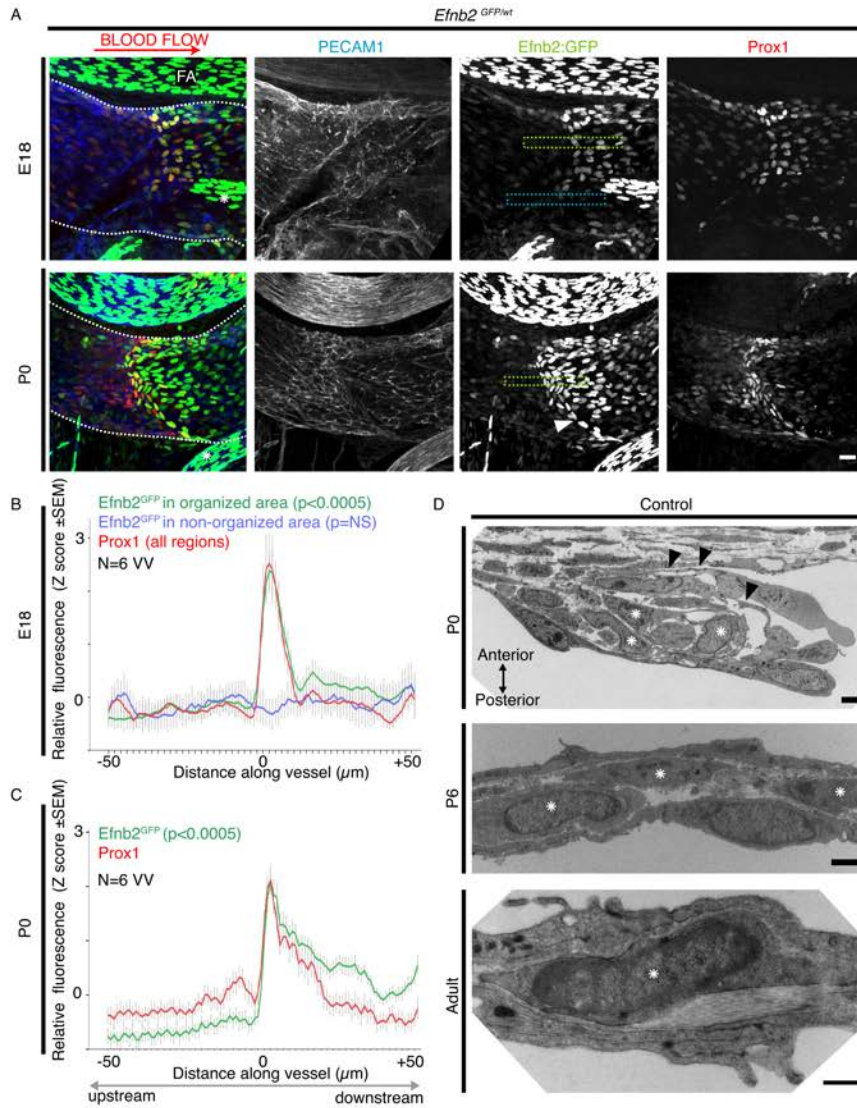
E) Bar chart shows the proportion of VVs identified at each stage, with stage and colour indicated in adjacent key, at P6 for the indicated genotypes. The number of VVs analysed for each condition is given above each bar.

1016    ****=P<0.00005, Chi Sq vs control, N=13 control VVs vs 10 Ephb4 deleted. Bars in

1017    A,C,D = 20μm

1018

1019

**Figure 4**

**Figure 4: Formation of ephrinB2 expression boundary in VV-forming region**

A) Localisation of PECAM1 (blue), Prox1 (red) and Efnb2GFP reporter signal (green, His-tagged and therefore nuclear) at E18 and P0 in heterozygous Efnb2GFP mice. Wholemount preparation of the proximal femoral vein is shown. At E18 there was partial, and variable, organization of VFCs. For example, in the superior area of the VV-forming region but not the inferior area. Those areas with organization at E18 showed a weak Efnb2GFP expression boundary, which was clearer at P0 (white arrowhead). Dotted lines indicate the femoral vein boundary, adjacent to the femoral artery (FA). As expected, arterial ECs showed stronger Efnb2GFP signal. ∗ indicates an overlying arterial branch (cut).

B-C) At E18, analysis of the relative fluorescence intensity across developing valves revealed a peak in Efnb2GFP signal (green line) coincident with that of Prox1hi (red) VFCs in organizing areas, but not in adjacent areas that are not yet organized (blue line). At both E18 and P0, Efnb2GFP signal is stronger downstream, and this difference is more apparent at P0. Mean of 6 VVs and 7-12 regions analysed per VV and representative regions analysed are shown boxed (green, blue) in A. P values in B,C are T tests comparing Efnb2GFP proximal and distal to the VFC leading edge. NS = not significant.

D) TEM analysis at P0 showed rotated VFCs detached from underlying basement membrane (arrowheads). Interstitial cells (∗) populated the developing leaflet core, and persisted at P6 and in adults. TEM micrographs are orientated at $90^{\circ}$ to confocal images, as indicated by arrows at P0 in D. Further examples of interstitial cells (in murine and human VVs) are shown in Supplementary Figure 3.

1048    N≥6 VV and blood flow left to right at all time points and in B,C. Bar = 20µm in A; and

1049    in D Bar = 2µm at P0-P6, 500nm in Adult.

1050

1051
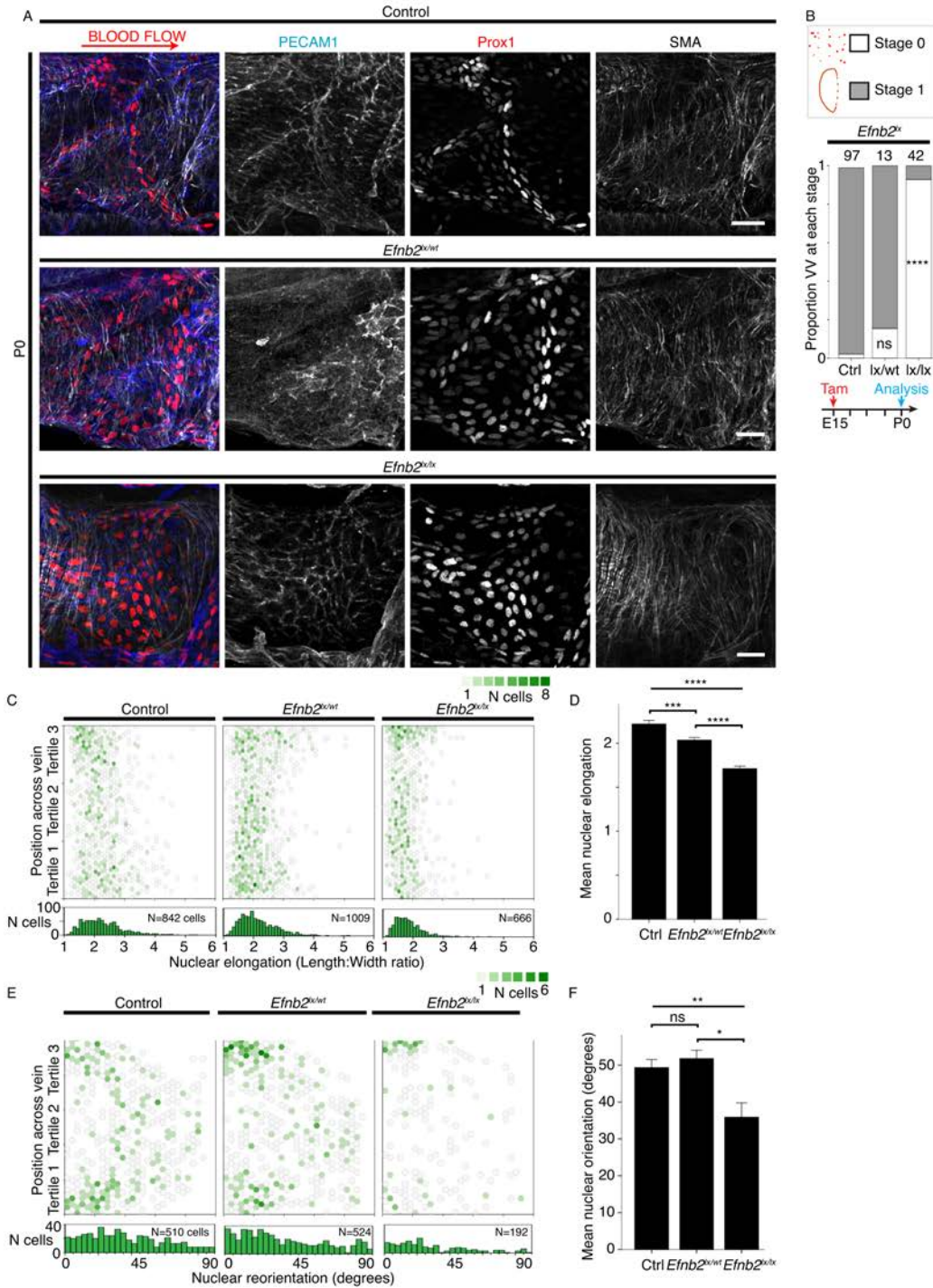
**Figure 5**

**Figure 5: Effect of *Efnb2* deletion on organization of VFCs**

1056

1057 A,B) Localisation of PECAM1 (blue), Prox1 (red) and SMA (white) in littermate

1058 controls, heterozygous (*Efnb2lx/wt*) and homozygous (*Efnb2lx/lx*) mice at P0,

1059 following Tamoxifen induction of Efnb2 deletion at E15. In controls and *Efnb2lx/wt*

1060 mice valves reached stage 1 of development, as normal. Homozygous deletion

1061 resulted in a failure to organize normally, with Prox1hi cells distributed over a wider

1062 upstream-downstream area of the vein, and failure of VFCs to elongate and

1063 reorientate.

1064 B) The bar chart shows the proportion of VVs identified at stage 0 (white) and stage 1

1065 (grey) at P0 for the indicated genotypes, and the number of VVs analysed for each

1066 condition is given above each bar. P values derive from two-sided Fisher's Exact test

1067 vs control.

1068 C) Hex-binned scatterplot of VFC elongation (length/width ratio) across the vein from

1069 superior to inferior. N=2517 cells, ≥6 VVs.

1070 D) Bar chart (±sem) summarising the results from (C) showing that both

1071 heterozygous and homozygous deletion resulted in significant reductions in VFC

1072 elongation. ANOVA with Bonferroni post hoc. For between groups ANOVA, F=109

1073 with 2df, P=3.2x10-46.

1074 E) Hex-binned scatterplot of VFC reorientation (in VFCs with nuclear length:width

1075 ratio ≥2) across the vein from superior to inferior. N=1226 cells, ≥6 VVs. After

1076 homozygous deletion, the VFCs with correctly reorientated nuclei were lost,

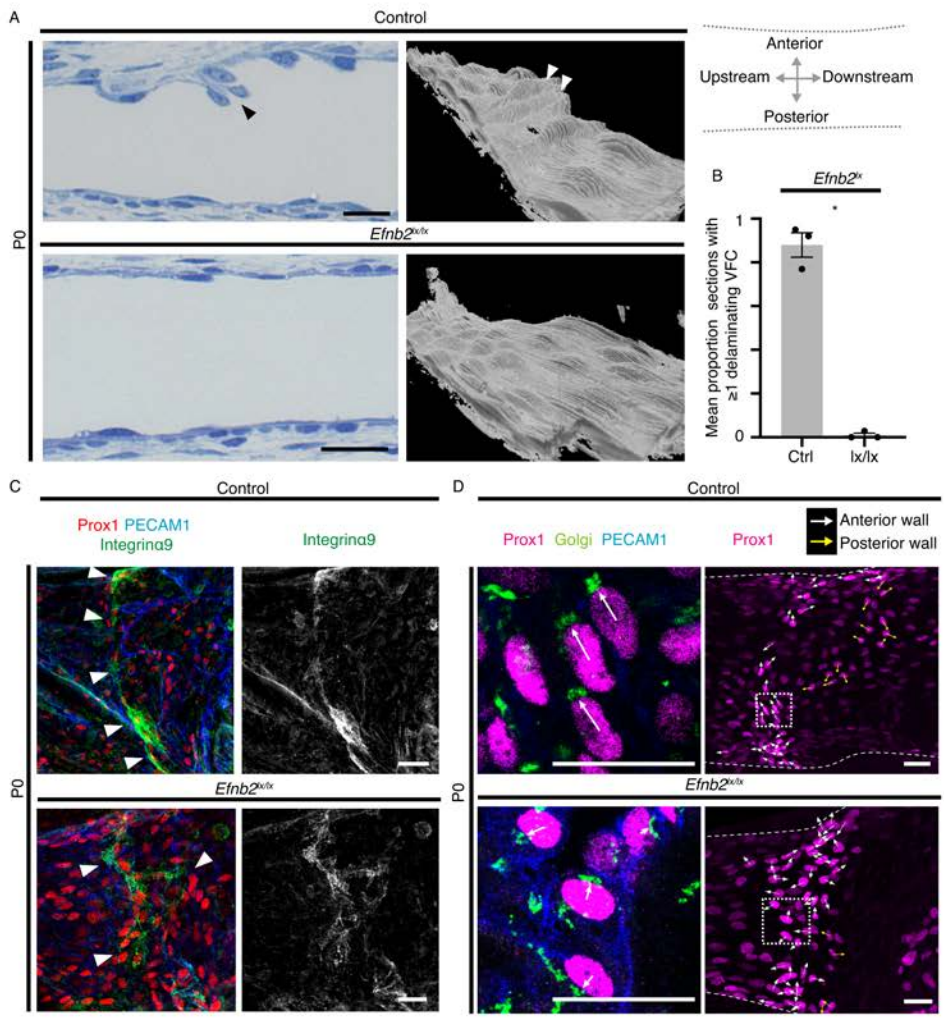1077 particularly in the centre of the vessel.

1078 F) Bar chart (±sem) summarising the results from (E). Homozygous deletion resulted

1079 in significantly reduced reorientation. ANOVA with Bonferroni post hoc. For ANOVA,

1080    F=7.1 with 2df, P=0.0009. *=P<0.05, **=P<0.005, ***P<0.0005, ****=P<0.00005.

1081    Bars = 20µm

1082

1083

1084 **Figure 6**

1085
1086

53

**Figure 6: Failure of VFCs to project into vessel lumen and abnormal integrin**

**expression**

A) Semi-thin longitudinal sections of P0 femoral veins showed protruding VFCs in littermate controls, but no protruding cells were seen after homozygous *Efnb2* deletion. 3D reconstructions of semi-thin sections show protruding VFCs (arrowheads) in controls only. The schematic indicates the orientation of the semi-thin sections.

B) A significant reduction in the mean number of sections showing protruding cells was identified. (≥60 sections were analysed per sample, T test, N=3 VV per group, error bars indicate SEM).

C) Integrinα9 was expressed in a ring around the organized VFCs in littermate controls (white arrowheads), but after homozygous *Efnb2* deletion, the localisation of integrinα9 expression was disrupted and chaotic (P<0.05, Chi Square test of the proportion of VVs showing normal vs disrupted integrinα9 expression pattern, N≥6 VV per group)

D) VFC polarity (indicated by white arrows) was examined by co-staining for Prox1 (magenta), PECAM1 (blue) and Golgi (green). Polarity was determined for individual VFCs using 0.5µm sections, and a z-projection of 2-4 confocal sections shown on the right (area enlarged outlined by dotted box,). In littermate controls, cells in the central region of the vein were aligned with the line of organized VFCs, whilst after homozygous *Efnb2* deletion, cell alignment was chaotic. P<0.05, Chi Square test of
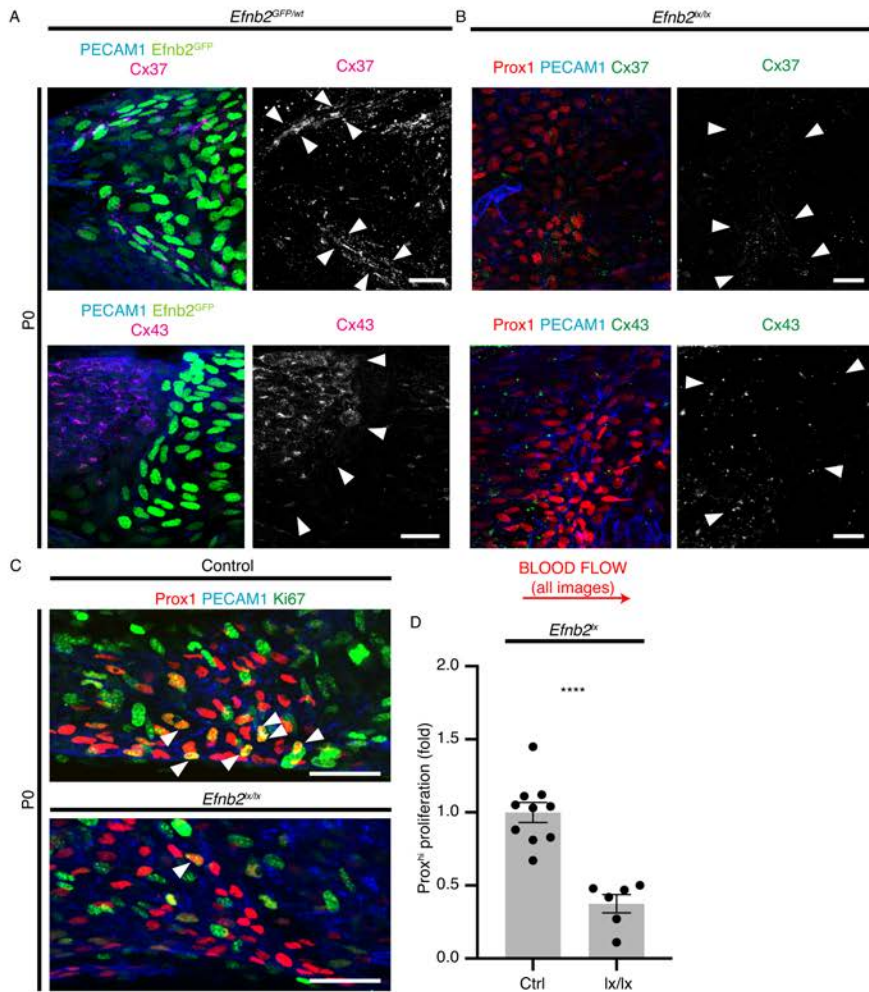
1112    the proportion of VVs showing normal vs chaotic VFC alignment, N≥8 VV per group.

1113    Yellow arrows indicate VFCs on the posterior vein wall. Bars in A,C,D 20µm. C and D

1114    are oriented as shown in Fig.2A.

1115

1116

**Figure 7**

1120 **Figure 7: *Efnb2* deletion disrupts gap junction protein expression pattern, and**

1121 **proliferation**

1122

1123 A) Localisation of PECAM1 (blue), and either Cx37 or Cx43, as indicated (magenta)

1124 around VFCs at P0 in heterozygous Efnb2GFP (green) mice. As expected, at P0

1125 Cx37 was localised to Efnb2GFP-expressing VFCs, primarily forming large gap

1126 junction plaques (examples indicated between arrowheads) and Cx43 was localised

1127 to endothelium upstream of these VFCs (region to the left of the arrowheads).

1128 Smaller plaques are also identifiable.

1129

1130 B) Localisation of PECAM1 (blue), Prox1 (red) and either Cx37 or Cx43, as indicated

1131 (green), after homozygous deletion of *Efnb2*. The tightly regulated expression pattern

1132 of Cx37 was disrupted, with expression over a wider area (arrowheads) and the

1133 typical appearance of larger plaques was lost. The expression pattern of Cx43 was

1134 also disrupted and no longer confined to upstream of VFCs (arrowheads). ($P<0.05$,

1135 Chi Square test of the proportion of VVs showing normal (confined) vs disrupted

1136 expression pattern, N≥6 VV per group).

1137 C-D) The proportion of proliferating VFCs was assessed by colocalisation of Prox1

1138 and Ki67 (arrowheads). Ki67+ve VFCs were easily identified in littermate controls,

1139 but far fewer proliferating VFCs were identifiable after homozygous *Efnb2* deletion.

1140 The inferior region of the vein is shown. ($P<0.00005$, unpaired T test, N≥6 VV per

1141 group, error bars indicate SEM). Bars in A-C = 20µm

1142